8. SITE 559[1]

Shipboard Scientific Party[2]

HOLE 559

Date occupied: 14 October 1981

Date departed: 16 October 1981

Time on hole: 52 hr.

Position (latitude; longitude): 35°07.45′N; 40°55.00′W

Water depth (sea level; corrected m, echo-sounding): 3754

Water depth (rig floor; corrected m, echo-sounding): 3764

Bottom felt (m, drill pipe): 3766

Penetration (m): 301

Number of cores: 8

Total length of cored section (m): 63.0

Total core recovered (m): 23.5

Core recovery (%): 37.3

Oldest sediment cored:
Depth sub-bottom (m): 249
Nature: Limestone
Age: middle Miocene

Basement:
Depth sub-bottom (m): 238
Nature: Basalt

Principal results: Hole 559 (Site MAR-8) was drilled between Anomalies 12 and 13 on the west flank of the Mid-Atlantic Ridge midway between Oceanographer and Hayes fracture zones (Fig. 1). The sediments were washed down to basement, which was felt at 238 m sub-bottom.

Aphyric pillow basalts were cored through the entire 63-m basement section. The principal macroscopic features are the variability in degree of alteration and the large amount of fresh glass recovered. These basalts belong to a single petrographic chemical group. The effects of alteration are clearly shown by chemical data. The observed variations in Sr are due in part to contamination induced by alteration. These variations can be used for choosing samples whose inferred Sr contamination is less than 5 ppm for Sr isotopic studies. The Sr concentration in fresh glass is 157 ppm.

Magmaphile element concentrations are enriched relative to chondrites (Nb = 16, Zr = 100, Ti = 9000, Y = 35, and V = 300 ppm). Although this result agrees with the hypothesis of a boundary at the latitude of Hayes Fracture Zone, no definite conclusion can be made because of the complexities revealed at Sites 558 and 556 on the same isochron.

The following analyses were not done for Site 559: sediment accumulation rates, pore water chemistry, and downhole measurements.

OPERATIONS

Approach to Site

After analyzing the results of drilling at Site 558, we decided to drill Site 559 near the original location of MAR-8 between Anomalies 12 and 13 south of the Oceanographer Fracture Zone. A tentative site was located, based on existing magnetics data, halfway between two smaller fracture zones that are themselves sandwiched by the Hayes and Oceanographer fracture zones.

The initial approach to the site began at 0220Z on 14 October (Fig. 2) on a track parallel to the fracture zones and crossing the prime target area. Although in general the basement relief was quite variable and the sediment cover was greater than 0.5 s, a location was observed at 0353Z (Fig. 3) where the sediment cover thinned to less than 0.25 s on the flank of a small basement high. Profiling was continued for 4 miles beyond this point until the location of Anomaly 13 was confirmed. The ship's course was then reversed and the site relocated. The beacon was dropped on Site 559 at 0518Z.

On-Site Operations

Site 559 was spudded at 1238Z 14 October in 3766 m of water. Sediments were washed to a depth of 238 m sub-bottom where basement was reached. Between 1930Z 14 October and 2230Z 15 October, 63 m of basement were cored without any major problems (Table 1). Drilling was then discontinued because of time considerations. The *Challenger* was under way to Site 560 at 0730Z 16 October.

SEDIMENT LITHOLOGY

At Site 559 the sediments were washed to basement at 238 m. At that time a wash core was retrieved that contained 2 m of disturbed marly nannofossil ooze (white 2.5YN 8 and 10YR 8/2) and marly nannofossil ooze with volcanic glass. The core includes upper Pliocene to upper middle Miocene sediments. No bioturbation or bedding was observed, except for faint color changes.

The sediment components are calcareous nannofossils (20–40%), clay (35–55%), foraminifers (3–15%), unspecified carbonate (5–10%), trace amounts to 10% of volcanic-derived material, and micronodules. In 559-

[1] Bougault, H., Cande, S. C., et al., *Init. Repts. DSDP*, 82: Washington (U.S. Govt. Printing Office).

[2] Henri Bougault (Co-Chief Scientist), IFREMER (formerly CNEXO), Centre de Brest, B. P. 337 29273 Brest Cedex, France; Steven C. Cande (Co-Chief Scientist), Lamont-Doherty Geological Observatory, Columbia University, Palisades, New York; Joyce Brannon, Department of Earth and Planetary Sciences, Washington University, St. Louis, Missouri, David M. Christie, Hawaii Institute of Geophysics, University of Hawaii at Manoa, Honolulu, Hawaii; Murlene Clark, Department of Geology, Florida State University, Tallahassee, Florida; Doris M. Curtis, Curtis and Echols, Geological Consultants, Houston, Texas; Natalie Drake, Department of Geology, University of Massachusetts, Amherst, Massachusetts; Dorothy Echols, Department of Earth and Planetary Sciences, Washington University, St. Louis, Missouri (present address: Curtis and Echols, Geological Consultants, 800 Anderson, Houston, Texas 77401); Ian Ashley Hill, Department of Geology, University of Leicester, Leicester LEI 7RH, United Kingdom; M. Javed Khan, Lamont-Doherty Geological Observatory, Columbia University, Palisades, New York (present address: Department of Geology, Peshawar University, Peshawar, Pakistan); William Mills, Deep Sea Drilling Project, Scripps Institution of Oceanography, La Jolla, California (present address: Ocean Drilling Program, Texas A&M University, College Station, Texas 77843); Rolf Neuser, Institut für Geologie, Ruhr Universität Bochum, 4630 Bochum 1, Federal Republic of Germany; Marion Rideout, Graduate School of Oceanography, University of Rhode Island, Kingston, Rhode Island (present address: Department of Geology, Rice University, P.O. Box 1892, Houston, Texas 77251); and Barry L. Weaver, Department of Geology, University of Leicester, Leicester, LEI 7RH, United Kingdom (present address: School of Geology and Geophysics, University of Oklahoma, Norman, Oklahoma 73019).

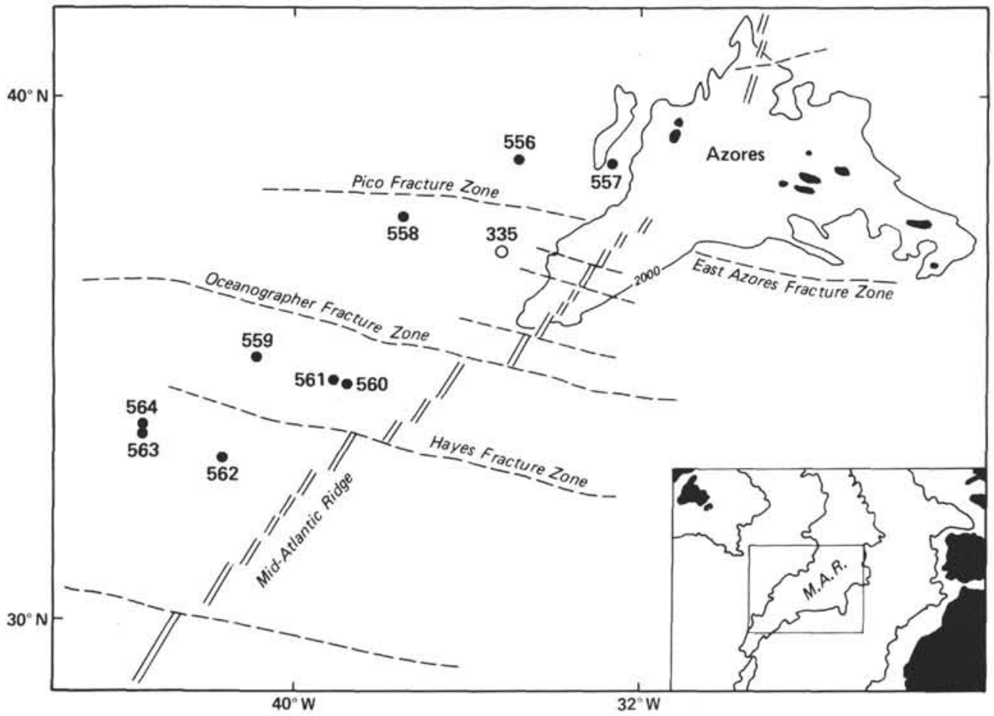

Figure 1. Site location map for Leg 82.

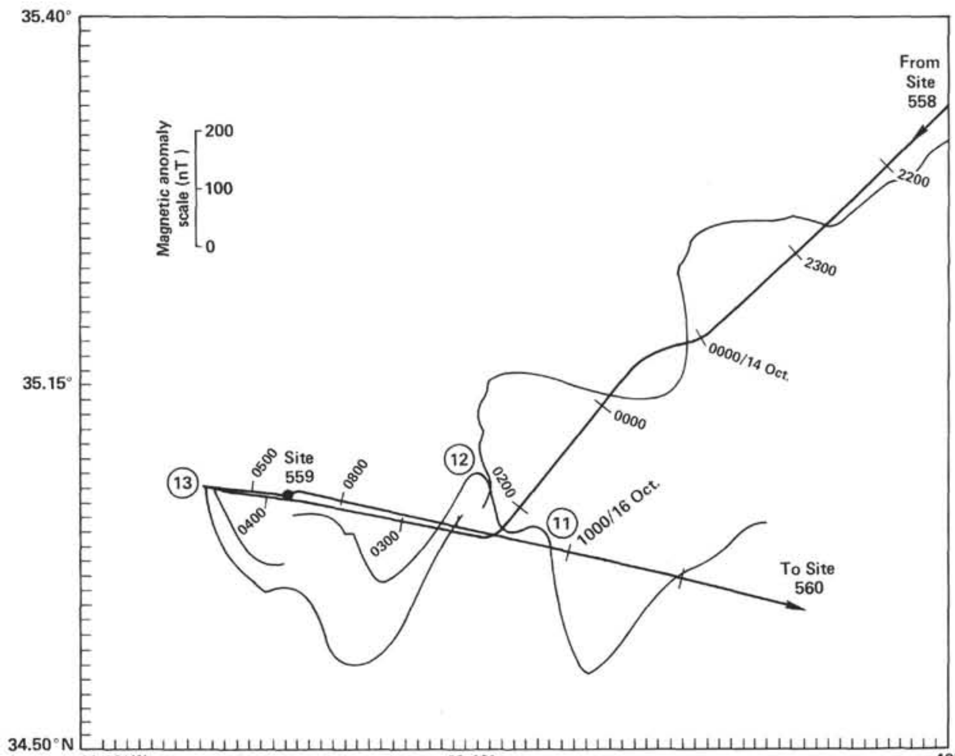

Figure 2. Approach and site survey track for Site 559. Heavy line is ship track with hour marks in GMT. Thin line is magnetic anomaly projected perpendicularly from the ship's track. Circled numbers are magnetic anomalies based on work at Lamont-Doherty Geological Observatory.

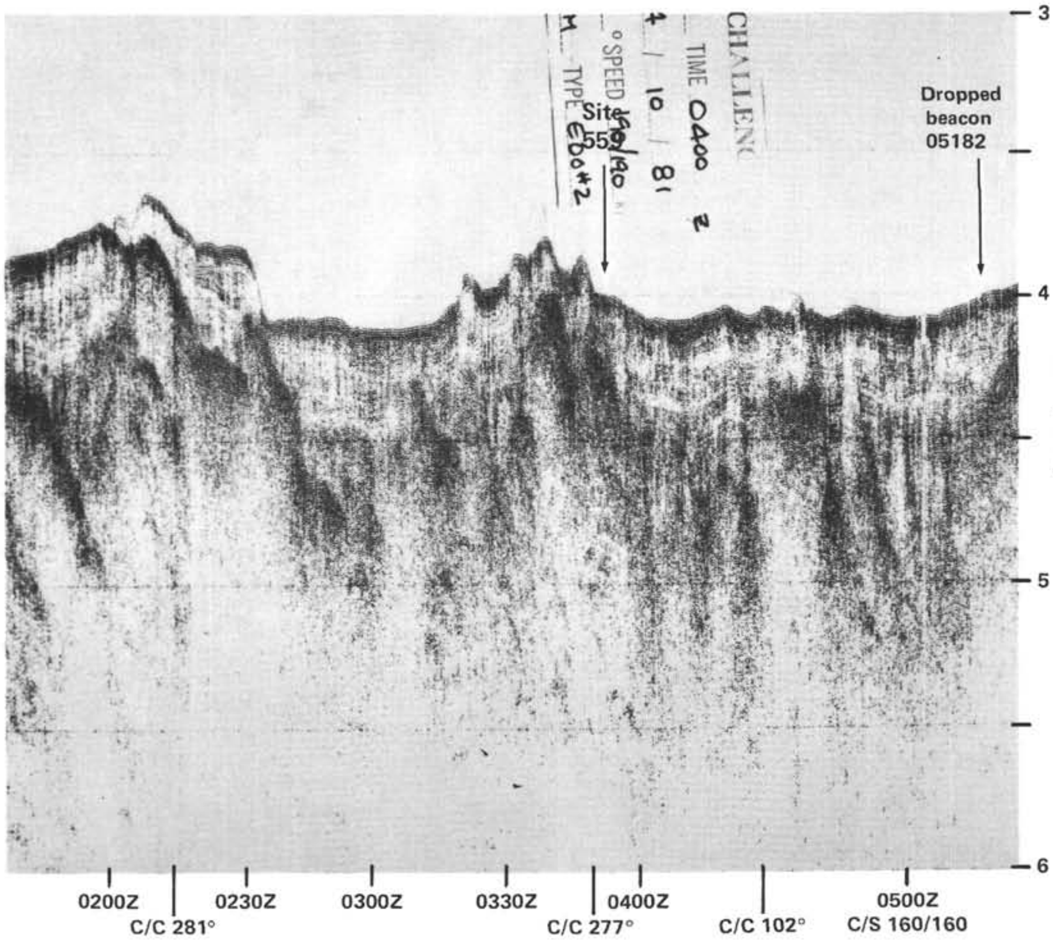

Figure 3. *Glomar Challenger* seismic profile over Site 559. For location of profile, see Figure 2. C/C = course change.

Table 1. Coring summary, Hole 559.

Core	Date (Oct. 1981)	Time (z)	Depth from drill floor (m)	Depth below seafloor (m)	Length cored (m)	Length recovered (m)	Percent recovered
H1	14	1605	3766.0–4004.0	0.0–238.0	0.0	0.00	0
1	14	2225	4004.0–4013.0	238.0–247.0	9.0	3.99	44
2	15	0310	4013.0–4022.0	247.0–256.0	9.0	3.82	42
3	15	0510	4022.0–4022.5	256.0–256.5	0.5	0.25	50
4	15	0920	4022.5–4031.0	256.5–265.0	8.5	2.72	32
5	15	1220	4031.0–4040.0	265.0–274.0	9.0	3.39	38
6	15	1550	4040.0–4049.0	274.0–283.0	9.0	2.60	29
7	15	1930	4049.0–4058.0	283.0–292.0	9.0	3.47	39
8	15	2230	4058.0–4067.0	292.0–301.0	9.0	3.27	36
					63.0	23.51	37

H1-2, 20 cm there is a thin layer of volcanic glass (moderately disturbed). As in Hole 558, traces of authigenic dolomite rhombs are present. The sediments retrieved at this site represent Neogene ocean pelagic sedimentation beginning in middle Miocene time.

Throughout the basalt units, intrapillow basalt (volcaniclastic) limestone is common. It occurs either between pillow margins or as fillings in basalt cracks and vesicles. Geopetal structures were observed in some vesicles. The limestones are moderately bioturbated and occasionally show inclined bedding contacts. Colors vary from very pale brown (10YR 8/3) to pale brown (10YR 6/3) and light gray (5YR 7/1) to pinkish white (5YR 8/2). Volcaniclasts are derived from adjacent vitric rims of pillow basalts. The original calcareous pelagic ooze has been recrystallized to micritic calcite, although ghosts of foraminifers still persist. The limestones in places are intensely mineralized by manganese oxide (usually dendritic) and are commonly veined by sparry calcite.

BIOSTRATIGRAPHY

Summary

Sediments for microfossil study from Hole 559 are wash cores. Based on the calcareous nannofossils, the age of the sediment ranges from middle Miocene to late Pliocene. One tentative determination based on poorly preserved nannofossils in Core 2 from a sediment streak below basement may be Oligocene.

Foraminifers in the wash core are from the latest Miocene to earliest Pliocene times. Although well preserved, they are not considered reliable age determinants.

Calcareous Nannofossils

Hole 559 was washed down to a depth of 238 m where basement material was encountered. Core H1 contains abundant and well-preserved nannofossils. *Discoaster brouweri* and *D. surculus* without *Reticulofenestra pseudoumbilica* occur in 559-H1-1, 14 cm. This suggests the upper Pliocene *D. brouweri* Zone, *D. surculus* Subzone

CN12b (NN16) for this sample. Sample 559-H1-2, 50 cm (slightly above the first basement material) is attributed to the *D. hamatus* Zone CN7 (NN9) because of the presence of *D. hamatus* and *D. neohamatus*.

A layer of sediment below basement level (Core 2) contains very poorly preserved nannofossils. A possible *Dictyococcites bisectus* and *Sphenolithus predistentus* are contained in this interval. Because they are so poorly preserved, these specimens are only tentatively identified. If these species do in fact occur, the sample could be lower Oligocene.

IGNEOUS PETROLOGY AND GEOCHEMISTRY

Hole 559 encountered basement at 238 m sub-bottom and penetrated 63 m of a single aphyric pillow basalt unit (Fig. 4). Basalts of this unit appear to belong to only one chemical group; a single, distinctive glass analysis may, however, indicate the existence of a second group.

Lithology

Pillow basalts of Site 559 are fine-grained, gray, aphyric basalts with localized small increases in grain size in the upper part and an overall grain-size increase downhole characterized by the presence of visible plagioclase needles (1-3 mm long) below about 286 m. Close to their margins, fine-grained pillow interiors grade over a few centimeters through a brown, altered variolitic zone to black aphanitic basalt and fresh glass. At the tops of most pillows, vesicles are abundant in the aphanitic zone and the outer few centimeters of the fine-grained zone. Two different types (generations?) of vesicles are present. Round vesicles up to 2 mm in diameter are commonly unfilled but may be calcite filled in altered zones. Larger, irregular vesicles up to 10 mm are calcite filled.

Fine-grained pillow interiors are largely weathered brown to brownish gray, particularly along fractures and calcite veinlets. Variolitic zones are generally altered light brown, but the outermost aphanitic basalt zones appear black and unaltered. Glass rims are generally fresh with only narrow palagonite rims along cracks and outer surfaces. Fractures and calcite-filled or limestone-filled veinlets are common throughout. Interpillow limestone is present above 266 m (Fig. 4).

Petrography

We examined seven thin sections of basalt from pillow interiors throughout the section. All are identical in primary mineralogy with only minor variations in grain size and texture. All contain interstitial zeolite (probably heulandite), replacing interstitial glass.

Site 559 basalts are composed of approximately 40% randomly oriented, elongate, hollow plagioclase laths (about An_{60}). Some anhedral, interstitial plagioclase is also present. Clinopyroxene occurs as relatively large prismatic grains (up to 0.5 mm), as parallel aggregates of smaller prisms and occasionally as sheaves or branching aggregates. Fresh olivine is present in only one sample, but relict outlines of small (1 mm) prismatic olivine grains, now completely altered to zeolite and brown clay, are always present (about 5%). Interstitial glass (about 25%)

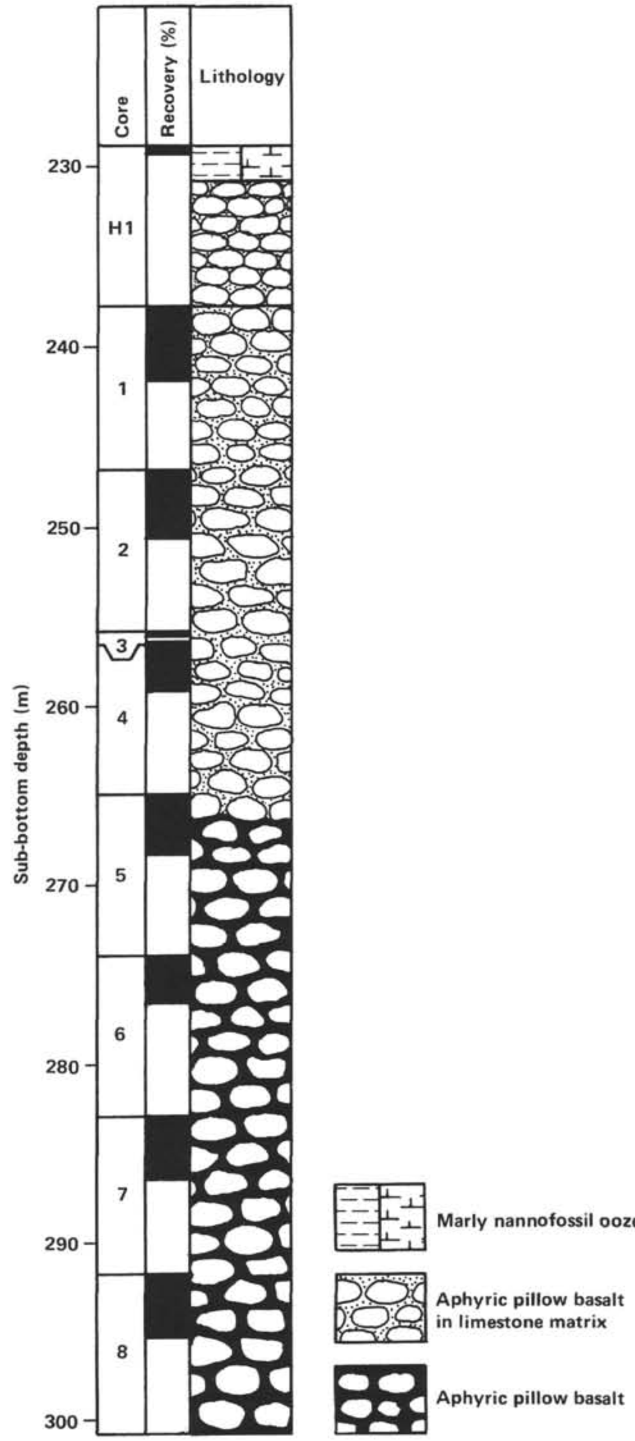

Figure 4. Basement lithology column, Hole 559.

has been partially (one sample) or completely replaced by colorless to light brown zeolite. This mineral occurs as aggregates of very fine, irregular, sometimes radiating grains with complex, sutured boundaries. Its low relief, moderately low birefringence (cf. quartz), straight or near-straight extinction, and length-slow character tentatively identify it as heulandite. Heulandite peaks are also present in the whole-rock X-ray diffraction pattern.

Heulandite is also present, with calcite, clay, and devitrified glass as vesicle fillings, and in some places it appears to have partly replaced plagioclase.

Geochemistry

Pillow basalts of Site 559 form a single lithologic unit as well as a single chemical group (Fig. 5). Analyses for glasses, pillow interiors, and altered outer zones of pillows are shown in Table 2.

In some cases, it was necessary to analyze altered outer zones of pillows (as evidenced by brown discoloration) because of a lack of fresh basalt in the core. In order to observe chemical changes resulting from this alteration, a pillow interior (559-1-2, 56–59 cm, [Piece 5C]) and an altered variolitic zone (559-1-2, 36–39 cm [Piece 5B]) of a single pillow were analyzed.

Changes in major element concentration (mole%), normalized to constant TiO_2 between the pillow interior and the altered variolitic zone are shown in Table 3. Relative to the assumed chemical immobility of such elements as Ti and Zr, significant chemical changes induced by alteration appear to be a decrease in SiO_2 and MgO and an increase in MnO, K_2O, P_2O_5, Sr, and V content. With the exception of the increase in P_2O_5, these changes are consistent with those observed in other comparative studies of alteration occurring at a low temperature (Mattey et al., 1981; Rice et al., 1979). These changes are comparable to those between the average of fresh pillow interiors and the average of altered basalts (shown in Table 4). Again, SiO_2 and MgO contents decrease, whereas MnO, K_2O, P_2O_5 and V increase. Because these visibly altered outer pillow areas are not representative of the fresher pillow interiors, we caution against the use of the altered outer pillow areas as representative samples of this chemical unit.

The chemical uniformity of fresh basalts at Site 559 is demonstrated by average statistical analysis of 15 pillow interiors, which are only slightly to moderately altered (Table 5). Average statistical analysis of seven visibly altered basalts is also given in Table 5.

Glassy pillow rims are abundant. Two distinct glass compositions are shown in Table 5. The average composition of three glasses is virtually identical to that of the average basalt. One glass (559-1-4, 20–22 cm [Piece 2]) is quite distinct in composition from all other samples at Site 559 (Fig. 5). It contains significantly less CaO, V,

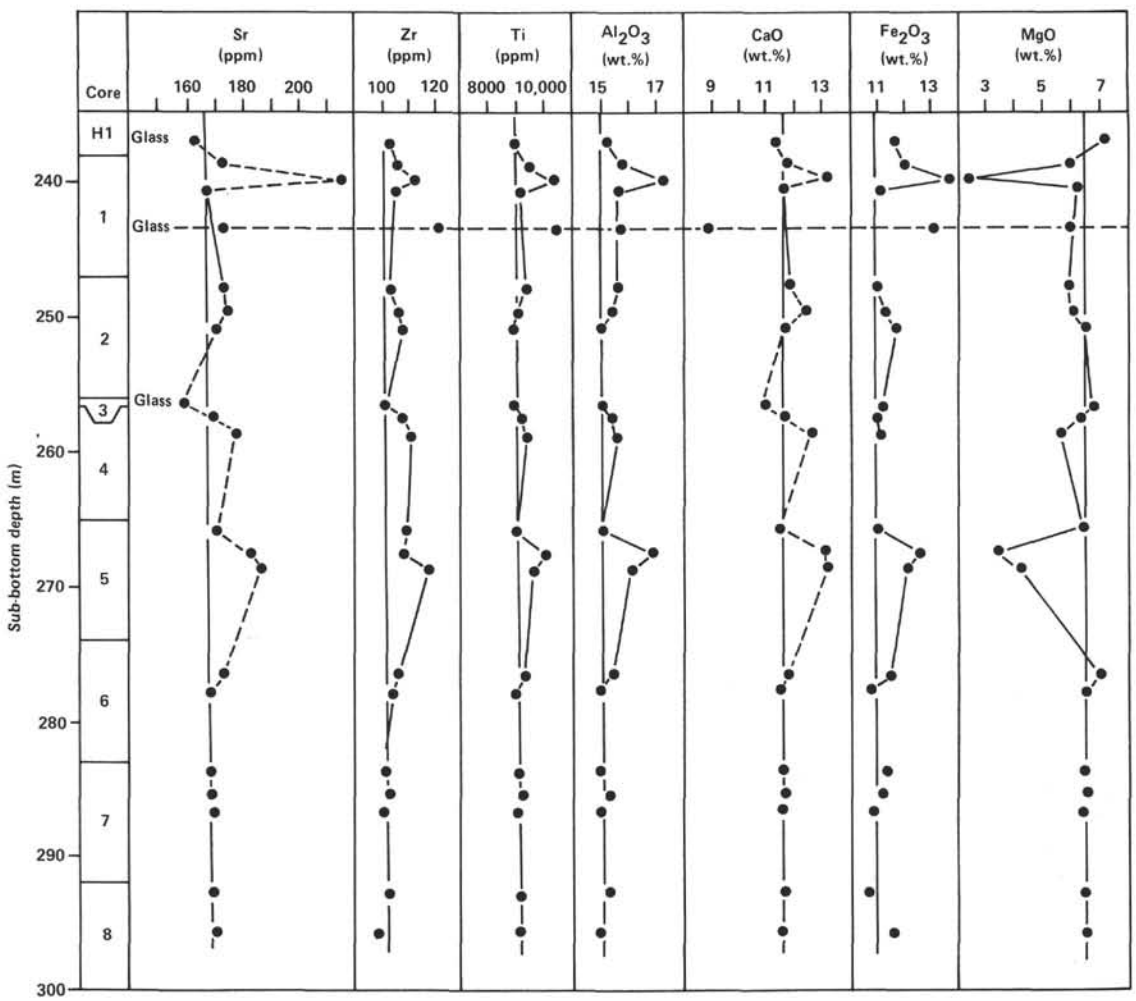

Figure 5. Downhole variations in chemical abundances, Hole 559. Some data appearing in Table 2 was not included in this figure because of the high degree of alteration.

Table 2. Analyses of major elements (in wt.%) and trace elements (in ppm) for Hole 559 basalts.

Core-Section (interval in cm) (piece number)	Depth (m)	Type of group	SiO_2	TiO_2	Al_2O_3	Fe_2O_3	MnO	Mg'	CaO	K_2O	P_2O_5	Total	Mg	Ti	V	Sr	Y	Zr	Nb
H1, CC (1)		G	50.62	1.49	15.20	11.70	0.18	8.29	11.32	0.30	0.19	99.29	61	8940	318	162	36.8	102	14.8
1-1, 120–123 (9B)	239.2	B	50.03	1.57	15.80	12.05	0.15	6.95	11.76	0.49	0.23	99.03	56	9420	317	172	37.3	105	17.5
1-2, 36–39 (5B)	239.8	AB	46.52	1.72	17.26	13.61	0.21	3.28	13.26	0.74	0.43	97.03	35	10,320	409	215	43.7	111	17.1
1-2, 56–59 (5C)	240.1	B	49.54	1.52	15.60	11.17	0.14	7.24	11.65	0.40	0.20	97.46	59	9120	305	166	36.4	104	15.2
1-3, 0–3 (1A)	241.0	AB	47.34	1.69	17.31	12.81	0.21	4.38	11.23	0.89	0.37	96.23	43	10,140	341	181	37.6	108	15.7
1-3, 44–47 (3B)	241.5	AB	46.70	1.60	16.59	12.31	0.16	3.97	14.15	0.64	0.29	96.41	42	9600	374	199	37.0	108	17.3
1-3, 76–79 (5A)	241.8	AB	48.16	1.58	15.94	11.83	0.18	5.22	13.19	0.38	0.26	96.74	50	9480	404	200	45.8	110	17.4
1-3, 129–132 (8C)	242.3	AB	47.82	1.69	16.93	12.79	0.23	5.91	12.97	0.50	0.29	97.13	41	10,140	404	187	39.2	108	14.9
1-3, 148–150 (9)	242.5	G	49.86	1.49	14.63	11.40	0.18	7.94	10.88	0.37	0.19	96.94	61	8940	301	157	33.4	101	16.0
1-4, 20–22 (2)	242.7	G	48.96	1.74	15.65	13.12	0.18	7.00	8.89	0.97	0.16	96.67	55	10,440	243	172	32.5	119	18.4
2-1, 1–3 (1A)	247.0	B	49.93	1.55	15.62	11.06	0.14	6.93	11.88	0.38	0.20	97.69	58	9300	304	172	35.9	102	16.9
2-2 24–28 (1B)	248.8	B	48.90	1.50	15.31	11.36	0.16	7.08	12.45	0.40	0.17	97.33	58	9000	248	173	33.6	105	16.1
2-3, 75–79 (4C)	250.8	B	49.80	1.47	14.91	11.78	0.17	7.55	11.78	0.49	0.18	98.13	59	8820	288	169	36.3	106	16.6
3-1, 13–14 (2)	256.1	G	50.35	1.48	15.02	11.25	0.18	7.81	10.92	0.40	0.18	97.19	61	8880	301	157	33.9	100	16.5
4-1, 125–129 (9B)	257.7	B	50.35	1.52	15.33	11.02	0.14	7.36	11.63	0.34	0.21	97.90	60	9120	300	168	35.3	106	16.0
4-2, 92–96 (5D)	258.9	B	49.42	1.54	15.47	11.15	0.15	6.67	12.76	0.43	0.20	97.79	57	9240	302	176	37.9	109	16.7
5-1, 45–48 (3B)	265.5	B	49.59	1.49	14.98	11.05	0.14	7.44	11.45	0.36	0.19	96.69	60	8940	283	169	35.4	97	15.5
5-2, 35–39 (4A)	266.8	AB	47.86	1.66	16.76	12.59	0.16	4.38	13.09	0.34	0.26	97.10	44	9960	369	181	37.3	106	16.7
5-3, 25–29 (2)	268.3	AB	48.72	1.58	16.01	12.11	0.15	5.10	13.19	0.44	0.23	97.53	49	9480	352	185	39.1	115	17.6
6-2, 25–29 (1B)	275.8	B	50.02	1.52	15.33	11.51	0.16	8.01	11.73	0.39	0.20	98.87	61	9120	314	171	36.0	104	15.3
6-3, 27–31 (1)	277.3	B	50.00	1.47	14.87	10.86	0.14	7.58	11.47	0.38	0.19	96.96	61	8820	298	167	35.9	102	16.3
7-1, 137–140 (12D)	284.4	B	49.67	1.49	14.81	11.33	0.17	7.46	11.55	0.42	0.19	97.09	60	8940	290	166	35.1	99	16.1
7-2, 143–146 (8C)	286.0	B	49.66	1.51	15.14	11.20	0.16	7.49	11.61	0.35	0.19	97.31	60	9060	307	166	35.3	100	15.8
7-3, 110–113 (7B)	287.1	B	50.06	1.48	14.84	10.90	0.14	7.34	11.54	0.34	0.18	96.82	60	8880	297	167	34.6	98	14.0
8-1, 48–51 (1B)	292.5	B	50.22	1.50	15.10	10.66	0.14	7.39	11.60	0.31	0.18	97.10	61	9000	304	167	34.0	100	16.1
8-3, 19–21 (1A)	295.2	B	49.96	1.49	14.80	11.51	0.15	7.46	11.44	0.41	0.20	97.42	59	8940	284	168	34.5	96	15.6

Note: Group types: G = glass, B = basalt, AB = altered basalt. Mg' is the atomic ratio of 100 × (Mg/[Mg + Fe^{2+}]) calculated using an assumed Fe_2O_3/FeO of 0.15. Measurements were made on board using ignited samples. Onshore analyses show loss on ignition to be less than 1%. The concentrations listed in the tables of compiled data (Appendix at end of volume) include volatile contents. Total Fe as Fe_2O_3.

Table 3. Assessment of chemical change during alteration of a pillow rim.

Element	Pillow interior (mole%)	Altered rim (mole%)	Normalized rim (mole%)	Relative change (%)
SiO_2	56.4	56.0	45.8	−19
TiO_2	1.30	1.59	1.30	0
Al_2O_3	10.5	12.2	10.0	−5
Fe_2O_3	4.8	6.2	5.0	+4
MnO	0.13	0.21	0.17	+31
MgO	12.3	5.9	4.8	−61
CaO	14.2	17.1	14.0	−1
K_2O	0.29	0.57	0.47	+62
P_2O_5	0.10	0.22	0.18	+80
Total	100.01	99.93	81.7	−18

Note: Pillow interior sample is 559-1-2, 56–59 cm (Piece 5C); altered variolitic rim from same pillow is 559-1-2, 36–39 cm (Piece 5B); "normalized rim" composition is normalized to 1.3 mole% TiO_2 (interior value); "relative change" is the change between normalized rim and pillow interior (normalized rim–pillow interior)/pillow interior. Analyses assume TiO_2 immobility.

Table 4. Chemical changes during alteration based on average Site 559 compositions.

Element	Fresh (mole%)	Altered (mole%)	Normalized altered (mole%)	Relative change (%)
SiO_2	56.5	56.3	49.4	−12
TiO_2	1.29	1.47	1.29	0
Al_2O_3	10.2	11.7	10.3	−1
Fe_2O_3	4.8	5.6	4.9	+21
MnO	0.12	0.19	0.17	+42
MgO	12.4	7.6	6.7	−46
CaO	14.3	16.5	14.5	+1
K_2O	0.28	0.45	0.39	+39
P_2O_5	0.09	0.15	0.13	+44
Total	99.98	100.01	87.78	−12

Note: "Fresh" is average fresh pillow interior; "altered" is average altered basalt; "normalized altered" is average altered basalt normalized to 1.2 mole% TiO_2; "relative change" is change between normalized altered basalt and fresh.

and Y and more Fe_2O_3, K_2O, Zr, and Nb than the average basalt. This sample may be the only representative of a second, distinct chemical unit. Pillow interiors adjacent both above and below this 6 cm-diameter glass piece have compositions close to the average of Site 559. No crystalline basalt analyzed at Site 559 has this unique glass composition. Further investigation of this sample is certainly required.

The relatively fresh sample (559-1-2, 56–59 cm [Piece 5C]) of the interior of a pillow and the strongly altered sample of the variolitic zone of the same section (559-1-2, 36–39 cm [Piece 5B]) were chosen to study the effect of alteration on the major element composition. These two samples were also chosen to study the effect of alteration on the abundances of the trace elements that have been chosen to describe the enrichment or depletion of magmaphile elements in terms of mantle heterogeneity: Nb, Zr, Ti, Y, and V. Rare earth elements have already been shown to be immobile in slightly to moderately altered basalts during low-temperature alteration (Rice et al., 1979), as have non-rare-earth magmaphile elements (Joron et al., 1979). However, because of the importance of measuring these elements on board in order to test for mantle heterogeneity, it was absolutely necessary to demonstrate on samples of this hole that low-temperature alteration has not modified the relative abundances of these elements. In the altered sample (559-1-2, 36–39 cm [Piece 5B]), the concentrations are increased by a factor of 1.15 ± 0.05 relative to the fresh

Table 5. Average analyses of Site 559 basalts. Major elements expressed in wt.%; trace elements in ppm.

Element	Fresh basalt (15)		Altered basalt[a] (7)		Glass[b] (3)		Glass[c] (1)
	$\overline{X}$	S	$\overline{X}$	S	$\overline{X}$	S	
SiO_2	49.8	0.4	47.6	0.8	50.3	0.4	48.96
TiO_2	1.51	0.03	1.65	0.06	1.49	0.01	1.74
Al_2O_3	15.2	0.3	16.7	0.6	15.0	0.3	15.65
Fe_2O_3	11.2	0.4	12.6	0.6	11.5	0.2	13.12
MnO	0.15	0.07	0.19	0.03	0.18	0	0.18
Mg′	7.3	0.3	4.3	0.7	8.0	0.2	7.00
CaO	11.8	0.4	13.0	0.9	11.0	0.2	8.89
K_2O	0.39	0.05	0.6	0.2	0.36	0.05	0.97
P_2O_5	0.19	0.07	0.30	0.07	0.19	0.01	0.16
Ti	9000	200	9900	300	8920	30	10,440
V	300	20	380	30	310	10	243
Sr	169	3	190	10	159	3	172
Y	36	1	40	3	35	2	32.5
Zr	102	4	109	3	101	1	119
Nb	16.0	0.8	17	1	15.8	0.9	18.4
Mg	59	1	43	5	61	0	55

Note: Numbers in parentheses are number of analyses. $\overline{X}$ = mean; S = standard deviation (1σ). Mg′ is the atomic ratio of 100 × (Mg/[Mg + Fe^{2+}]) calculated using an assumed Fe_2O_3/FeO of 0.15. Averages are calculated from data listed in Table 2 and are rounded.
[a] Samples 559-1-2, 36–39 cm (Piece 5B); 559-5-2, 35–39 cm (Piece 4A); 559-5-3, 25–29 cm (Piece 2); 559-1-3, 0–3 cm (Piece 1A); 559-1-3, 44–47 cm (Piece 3B); 559-1-3, 76–79 cm (Piece 5A); and 559-1-3, 129–132 cm (Piece 8C).
[b] Samples 559-H1, CC (Piece 1); 559-3-1, 13–14 cm (Piece 2); and 559-1-3, 148–150 cm (Piece 9).
[c] Sample 559-1-4, 20–22 cm (Piece 2).

sample (559-1-2, 56–59 cm [Piece 5C]), except for V (for which the increase is somewhat higher). The factor 1.15 accounts for the leaching out of major elements (MgO, SiO_2), and its accuracy (0.05) relative to the different magmaphile trace elements agrees with the precision of the concentration measurements. Thus, the relative abundances of magmaphile elements investigated on board are not affected by low-temperature alteration. Their relative abundances can be interpreted in terms of mantle heterogeneity and/or melting processes.

Figure 6 illustrates the effects of low-temperature seawater alteration on strontium and calcium concentrations. As the degree of alteration increases, strontium concentration increases. The less-altered samples of Site 559 located at the bottom of the hole are grouped in the vicinity of 165 ppm Sr and 11.6 wt%. CaO. Altered samples, denoted by squares, show increasing Sr and CaO concentrations. Glass samples have the lowest Sr and CaO content; glass from Section 559-1-4 (the triangle) is again unique. The two glass samples collected within the basalt section (559-1-3 [Piece 9] and 559-3-1) have exactly the same CaO and Sr contents (10.9 wt.% and 157 ppm, respectively), whereas Core H1 collected at the sediment/basement interface shows slightly higher concentrations (11.3 wt.% and 162 ppm). "Fresh" glasses showing the lowest Ca-Sr concentration are a good indication of the lowest contamination in Sr for $^{87}Sr/^{86}Sr$ ratio measurements.

The following table shows calculated Sr isotopic ratios for various degrees of seawater contamination of a basalt that has an initial Sr concentration of 160 ppm and Sr isotopic ratio of 0.7020.

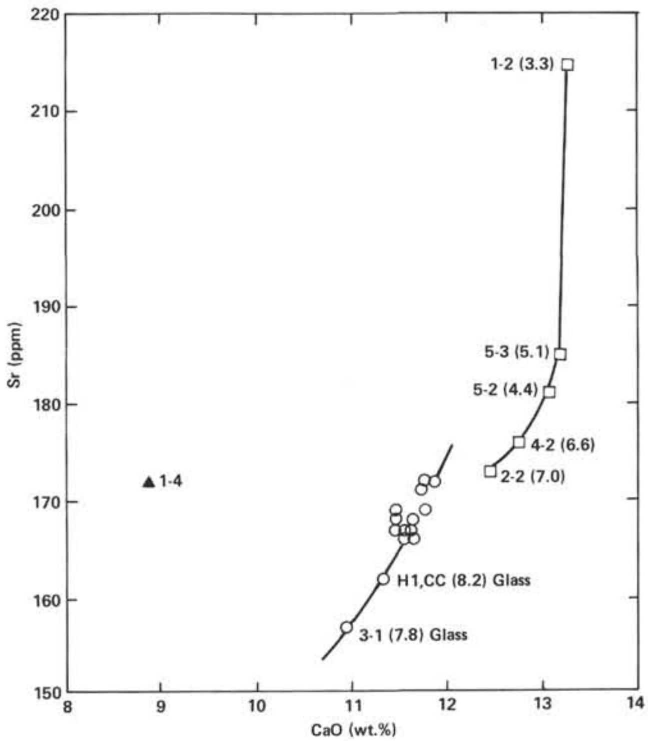

Figure 6. Sr versus CaO for altered and slightly altered basalts (squares) to unaltered basalts (circles). The triangle represents the unique glass sample (559-1-4, 20–22 cm [Piece 2]). Hyphenated numbers next to symbols represent Core-Section (in Hole 559); numbers in parentheses are Mg′-values (rounded to the nearest tenth) for these samples. Mg′ is the atomic ratio of 100 × (Mg/[Mg + Fe^{2+}]) calculated using an assumed Fe_2O_3/FeO of 0.15. Overly altered data in Table 2 has been excluded from this figure.

Seawater Sr added (ppm)	$^{87}Sr/^{86}Sr$
0	0.7020
1	0.7020
5	0.7022
10	0.7024
15	0.7026
20	0.7028
25	0.7029
30	0.7031

The Sr isotopic ratio can only be reliably interpreted as reflecting the mantle source composition if the amount of Sr added from seawater is lower than 5 ppm. To the extent that there is no Sr exchange between glass and seawater (which is a possibility mentioned by Rice et al., 1979), the lowest Sr concentrations (157 ppm) found in two glasses compared to 165 ppm in relatively fresh basalts allows us to postulate that the true concentration in Sr—and thus the true $^{87}Sr/^{86}Sr$ ratio—could be reached with a precision better than 5 ppm. In addition, care has to be taken in separating clean fragments of glass (1 mm size) and then leaching the powder with HCl or HNO_3 solution several times: the Sr concentration of the powder could be checked after each leaching by X-ray fluorescence measurements on the powder itself, until a constant value is found. The true Sr and $^{87}Sr/^{86}Sr$ could be reached this way only if glass-seawater exchange of Sr had occurred without other detectable modifications of the glass composition.

The extended Coryell-Masuda diagram is presented in Figure 7. The enriched pattern (Nb in respect to other elements) is typical of transitional basalts found in the Azores Triple Junction area. This result *by itself* would agree with a boundary between an Azores-type source north of Hayes Fracture Zone and a depleted source south of Hayes Fracture Zone. Nevertheless, the results obtained at Site 558 (where depleted, flat, and enriched patterns were found) force us to be cautious in any attempted interpretation of geochemistry and geodynamics. A confident interpretation of this type can only be made when we know why such different patterns are found at Site 558.

MAGNETICS

Basalt Paleomagnetism

Eight samples of basalt were taken for the study of paleomagnetic properties. The intensity of natural remanent magnetization and initial susceptibility were measured and Koenigsberger ratio (Q) calculated. The results are given in Table 6. Six samples have low intensity (0.1–0.8 × 10^{-3} emu/cm^3), whereas only two samples have high intensity values (1.0–1.3 × 10^{-3} emu/cm^3). Two samples from Sections 559-6-1 and 559-7-2 have the lowest intensities and also low Q values, but susceptibility values are moderate to high. Demagnetization was not done on board so that further properties could be studied onshore.

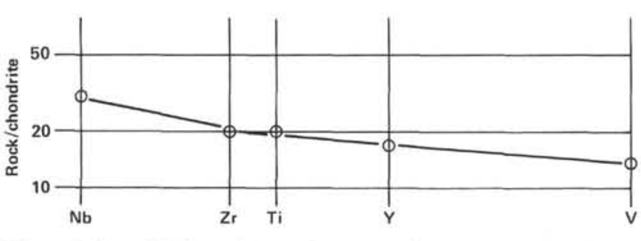

Figure 7. Extended Coryell-Masuda diagram for an average basalt composition, Hole 559.

The inclination values are shallower than the expected dipole inclination for the latitude of this site, which suggests tectonic rotation of the ocean crust since the acquisition of remanance. The negative values of inclination are in agreement with the location of this site between Anomalies 12 and 13.

PHYSICAL PROPERTIES

No sediment samples have been measured because no undisturbed sediment was recovered in the wash core. Samples from the basement cores were measured routinely for sonic velocity, density, and water content. The data are presented in Table 7.

Alteration of basalt specimens produces a wide range of densities and sonic velocities. Densities measured by the 2-minute GRAPE technique are systematically lower than those determined by the gravimetric technique. This is due to the core condition, which only allowed rather short minicores to be prepared. These were rather shorter than the minimum length (2.5 cm) required for an accurate determination by the GRAPE method. The limestone sediment with glass fragments measured from Section 559-1-4 has little acoustic impedance compared to the altered basalts, mainly because of its high sonic velocity of 3.84 km/s.

The data show no systematic variation down the hole.

SUMMARY AND CONCLUSIONS

Hole 559 is located between Anomalies 12 and 13 midway between the Oceanographer and Hayes fracture zones. The upper 63 m of the basement were cored and consist of aphyric pillow basalts belonging to a single magmatic unit. The effects of low-temperature alteration are variable and randomly distributed in the recovered samples. Fresh glasses are very common at the pillow margins; calcite is present in cracks and veins. MgO concentration (about 8% in fresh samples) decreases to 3% in badly altered samples. The loss of MgO and SiO_2 induces higher concentrations of other major elements and of magmaphile trace elements (e.g., Nb, Zr) in altered samples. We think that fresh glasses—which have a lower Sr concentration (157 ppm) than the freshest basalts (165 ppm)—should be suitable, after leaching processes, for Sr isotopic ratio measurements. A fresh glass sample with a different and unusual composition has been found (SiO_2 = 48.96, TiO_2 = 1.74, Al_2O_3 = 15.65, Fe_2O_3 = 13.12, Mg′ = 7.0, CaO = 8.89, and K_2O =

Table 6. Paleomagnetic properties, Hole 559.

Core-Section (interval in cm)	J_{NRM} (× 10^{-3} emu/cm^3)	NRM dec. (°)	NRM inc. (°)	χ (× 10^{-6} emu/cm^3 Oe)	Q (= $J_{NRM}/0.45\ \chi$)
1-2, 134–136	0.75	216.3	−32.7	72	23.15
2-1, 113–115	0.33	186.9	−22.9	65	11.28
4-2, 82–84	1.00	325.0	−29.5	76	29.24
6-1, 76–78	0.21	277.1	−22.2	84	5.56
7-2, 60–62	0.15	183.4	−27.0	64	5.21
7-3, 145–147	0.77	180.9	−26.9	94	18.20
8-1, 37–39	0.76	80.3	−7.0	58	29.12
8-3, 15–17	1.28	270.9	−22.9	64	44.44

Note: J_{NRM} = intensity of natural remanent magnetization (NRM); dec. = declination; inc. = inclination; χ = susceptibility; Q = Königsberger ratio.

Table 7. Physical properties, Hole 559.

Core-Section (interval in cm)	Sub-bottom depth (m)	Sonic velocity (km/s) V.	Sonic velocity (km/s) H.	Tempera-ture (°C)	Thermal conductivity (mcal/[cm · deg · s])	GRAPE density (g/cm^3) V.	GRAPE density (g/cm^3) H.	Gravimetric density: Wet-bulk density (g/cm^3)	Gravimetric density: Water content (%)	Gravimetric density: ϕ (%)	Acoustic impedance ($\times 10^5$ g/[cm·s])	Lithology or remarks
1-1, 93–107	239.0	4.73		22.0		2.55		2.7	5	14	12.8	Basalt
1-4, 0–7	242.5	3.84		22.0		2.24		2.4	8	20	9.2	Interpillow sediment
2-3, 93–107	251.0	4.52		22.0		2.55		2.6	7	17	11.8	Basalt
4-1, 35–37	256.9							2.8	<1	<1		Pillow basalt
5-3, 35–36	269.4							2.8	2	7		Basalt
6-1, 76–78	274.8	4.47		22.0		2.25(?)					10.1	Heavily altered basalt
6-2, 15–17	275.7							2.8	4	10	—	Basalt
7-2, 58–61	285.1	4.46		22.0		2.55					11.4	Altered basalt
7-2, 70–72	285.2							2.6	6	16	—	Altered basalt
8-3, 13–17	295.2	4.71		22.0		2.70		2.8	4	12	13.2	Basalt

Note: V. = vertical, H. = horizontal; water content is corrected; ϕ = porosity. All values measured at laboratory temperature and pressure. For details of techniques, see Explanatory Notes chapter (this volume).

0.97, all in wt.%). Site 559 is characterized by a typical enriched abundance pattern for magmaphile elements ($[Nb/Zr]_{ch} = 1.65$).

This result would agree with a geochemical boundary between an Azores-type source north of Hayes Fracture Zone and a depleted source south of Hayes Fracture Zone. Nevertheless, the results obtained at Site 558 (where enriched, flat, and depleted materials were found) necessitate further analyses before a definite interpretation can be made.

REFERENCES

Joron, J. L., Bollinger, C., Quisefit, J. P., Bougault, H., and Treuil, M., 1980. Trace elements in Cretaceous basalts at 25°N in the Atlantic Ocean: Alteration, mantle composition, and magmatic processes. *In* Donnelly, T. W., Francheteau, J., Bryan, W., Robinson, P., Flower, M., Salisbury, M., et al., *Init. Repts. DSDP*, 51, 52, 53, Pt. 2: Washington (U.S. Govt. Printing Office), 1087–1098.

Mattey, D. P., Marsh, N. G., and Tarney, J., 1981. The geochemistry, mineralogy, and petrology of basalts from the West Philippine and Parece Vela Basins and from the Palau-Kyushu and West Mariana Ridges, Deep Sea Drilling Project, Leg 59. *In* Kroenke, L., Scott, R., et al., *Init. Repts. DSDP*, 59: Washington (U.S. Govt. Printing Office), 753–800.

Rice, S., Langmuir, C. H., Bender, J. F., Hanson, G. N., Bence, A. E., and Taylor, S. R., 1980. Basalts from Deep Sea Drilling Project Holes 417A and 417D, fractionated melts and a light rare-earth depleted source. *In* Donnelly, T. W., Francheteau, J., Bryan, W., Robinson, P., Flower, M., Salisbury, M., et al., *Init. Repts. DSDP*, 51, 52, 53, Pt. 2: Washington (U.S. Govt. Printing Office), 1099–1112.

SITE 559 HOLE CORE H1 CORED INTERVAL 0.0–238.0 m

TIME – ROCK UNIT	BIOSTRATIGRAPHIC ZONE	FORAMINIFERS	NANNOFOSSILS	SECTION	METERS
upper Pliocene	CN12b (NN16)	N17/N18?		1	0.5, 1.0
lower Pliocene	CN10	AG			
upper Miocene	CN9b (NN11)		CN7–NN9	2	
middle Miocene	CN7 (NN9)		AG	CC	
			CN7/NN9 *Discoaster hamatus* zone		

GRAPHIC LITHOLOGY

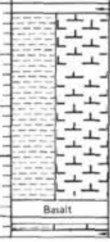

void
2.5Y N8
Volcanic glass in washed residue (for forams)
10YR 8/3 (volcanic glass)
10YR 8/2
basalt

LITHOLOGIC DESCRIPTION

Section 1, 10–60 cm: MARLY NANNO OOZE.

Section 1, 60 cm–Section 2, 20 cm: MARLY NANNO OOZE with volcanic glass.

DOMINANT LITHOLOGY MARLY NANNOFOSSIL OOZE

White (2.5Y N8), 10YR 8/2 in Section 2, 32–42 cm
Soft or soupy to firm
No bioturbation or bedding except sharp color change at Section 2, 20 cm, and faint color chanoe at Section 2, 32 cm.
Volcanic glass (black) and zeolites at contact Section 2, 20 cm.

Minor lithology:
Marly nanno ooze with volcanic glass
Marly limestone (CC), white (10YR 8/2) with slightly darker laminae.

Note: glass makes up about 5–10% of the material from Section 1, 60 cm to Section 2, 20 cm, but fragments are large and do not appear in smear slide analysis.

SMEAR SLIDE SUMMARY (%):

Composition:	1, 20	1, 55	1, 140	2,20	2,31	2, 40	CC
Feldspar	Tr	Tr	Tr	Tr	Tr	Tr	Tr
Heavy minerals	Tr	Tr	Tr	Tr	Tr	Tr	Tr
Clay	50	40	49	50	43	50	35–55
Volcanic glass	1	Tr	–	3	Tr	–	–
Palagonite	–	–	–	2	–	–	–
Micronodules	2	1	3	Tr	Tr	Tr	1–2
Zeolite	–	–	–	5	–	–	–
Carbonate unspec.	5	8	7	10	5	5	22–35
Foraminifers	5	9	8	8	15	3	–
Calc. nannofossils	35	40	30	20	35	40	20–28
Diatoms	1	Tr	1	Tr	–	Tr	Tr
Radiolarians	1	Tr	1	Tr	Tr	Tr	–
Sponge spicules	–	–	–	–	–	Tr	–
Dolomite	–	Tr	Tr–1	–	Tr?	Tr	Tr

SITE 559 HOLE CORE 1 CORED INTERVAL 238.0–247.0 m

SECTION	METERS
1	0.5, 1.0
2	
3	
4	

GRAPHIC LITHOLOGY

10YR 8/3
10YR 8/3
T 10YR 8/3
10YR 8/3
basalt

LITHOLOGIC DESCRIPTION

INTRAPILLOW-BASALT (VOLCANICLASTIC) LIMESTONE

Very pale brown (10YR 8/3). The volcaniclastic component increase towards the margin of the pillow basalts.

Manganese mineralization occurs throughout the limestones as micronodules or dendrites.

The micritic limestone has been recrystalized to irregular patches of microspar.

Throughout the pillow basalts sediment (now limestone) has infiltrated cracks and vesicle with the latter often showing geopetal structures.

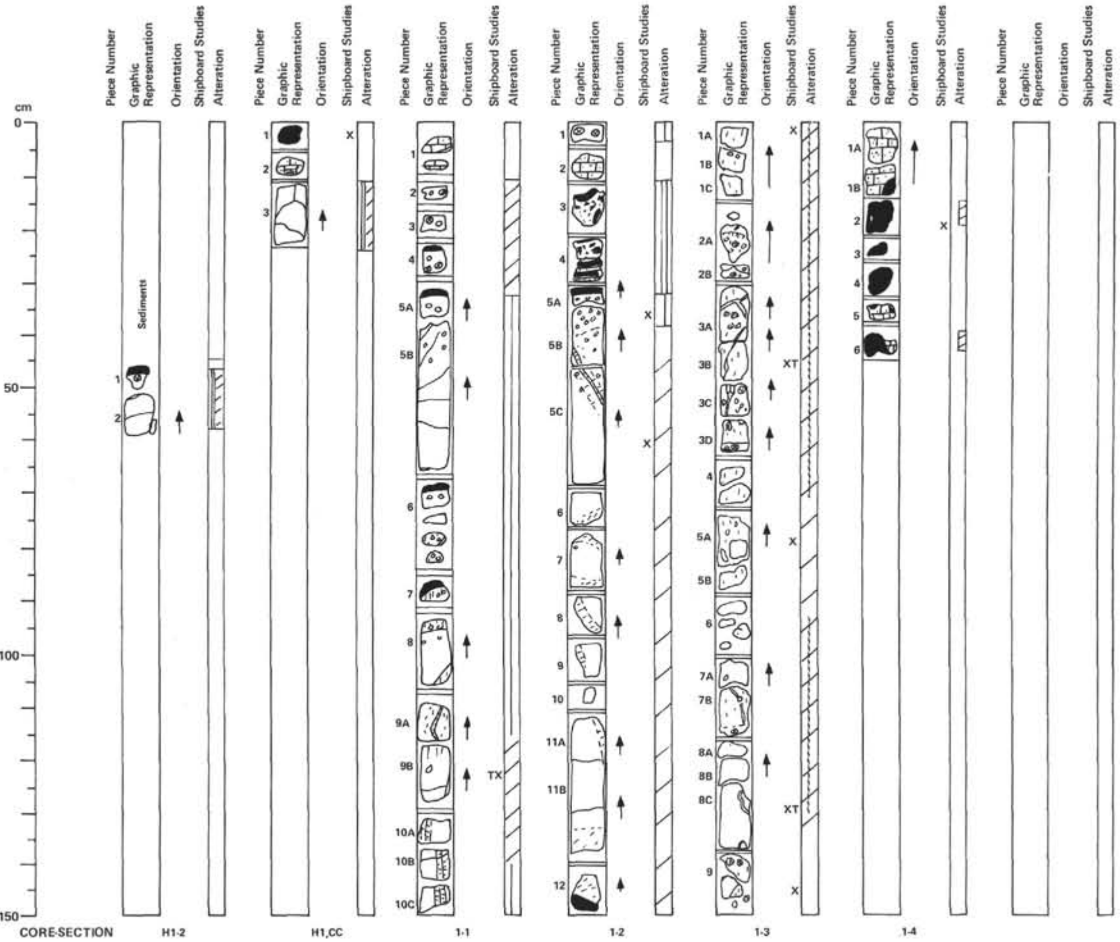

SITE 559, CORE H1 Depth 0.0–238.0 m

SECTION 2

APHYRIC PILLOW BASALT FRAGMENTS

Color dark brown (10YR 3/3) to brown (10YR 4/3); moderately to badly altered. Fresh black aphanitic to glassy basalt in Piece 1 with variolitic zone grading to altered basalt (size of varioles ≲1 mm). Vesicles are scattered throughout the rock (size <1 mm, few <3 mm) and often filled with calcite.

CORE-CATCHER

APHYRIC PILLOW BASALT FRAGMENTS

Pieces 1 and 3.

1–4 cm: Black vesicular basalt glass. Vesicles (≲1.5 mm) are round and empty.

7–10 cm: Limestone. One half is laminated.

13–23 cm: Moderately to badly altered aphyric basalt. Color brown to dark brown (10YR 4/3–10YR 3/3). Round vesicles (≲1.5) and irregular shaped vesicles (≲10 mm) are empty or calcite-filled. Some small veinlets are cemented by calcite, too.

SITE 559, CORE 1 Depth 238.0–247.0 m

SECTION 1

APHYRIC PILLOW BASALT SEQUENCE

0–10 cm: Limestone, very pale brown (10YR 8/3), dendrites throughout the limestone (MnO).

10–30 cm: Variolitic basalt, dark gray (2.5Y N4/0).

10–22 cm, Pieces 2 and 3: 30–40% vesicles, unfilled.

22–30 cm, Piece 4: Glass rim, 10% unfilled vesicles.

30–84 cm: Aphyric basalt, grayish brown (10YR 5/2), fine grained, highly altered, thin calcite filled fractures, round vesicles concentrated to 30% in Pieces 5A, 6 and the upper cm of Piece 5B.

84–150 cm: Aphyric basalt, dark gray (5Y 4/1), fine grained, alteration as noted at top of Pieces 7, 8, and 9B, and along fractures. Vertical fractures are filled with limestone sediment, horizontal fractures are filled with calcite. Unfilled round vesicles (≈1 mm) in Piece 7 and upper 2 cm of Piece 8. Weathered areas are brown (10YR 5/3). Pieces 5B, 6, and 8 contain irregular shaped vesicles (2–8 mm) filled with calcite.

Thin Section at 120–123 cm.

SECTION 2

APHYRIC PILLOW BASALTS

1–4 cm: Strongly altered variolitic aphyric basalt, color brown (10YR 5/3). Size of varioles ≲4 mm.

6–11 cm: Limestone, color pale brown (10YR 8/3). Black dendrites of Mn-Oxide are grown throughout the sediment.

14–29 cm: Basalt glass breccia (hyaloclastite); angular clasts (size ranges between 1 mm and several cm) of vesicular (round, ≲2 mm) sideromelane; fresh (black) in the center, altered (brown) at the rims. Matrix is limestone as above (Piece 2).

31–149 cm: Separate pillow of fine-grained aphyric basalt, color dark gray (10YR 4/1). High amount of round vesicles in upper part (Piece 5A and B), size ≲2 mm. From 41–52 cm: vein filled with lutitic limestone from above. Pieces 5A and 12: Fresh glass rims on aphanitic, black basalt.

SECTION 3

APHYRIC PILLOW BASALTS

Moderately to highly altered aphyric basalt (highly altered brown [10YR 5/3], moderately grading to dark grayish brown [10YR 4/2]). Two generations of vesicles suggested, esp. in 0–60 cm interval. Large vesicles 2–5 mm, calcite filled*, smaller empty ones ≲1 mm–2 mm in diameter. Pieces 2A, 3D, 7B, and 9 are dark gray (7.5YR N4/0) to very dark gray (7.5YR N5/0) aphanitic, aphyric basalt grading to altered variolitic brown basalt. Calcite veining is frequent and dominantly longitudinal. Absence of consolidated glass relative to Sections 1 and 4 is striking. relative to Sections 1 and 4 is striking.

*Some larger cavities are present with the longitudinal calcite veining, calcite lined, in Pieces 1A–C, 3C, 7B, and 8C).

SECTION 4

BASALT GLASS AND LIMESTONE

0–13.5, 35–38, and 43–45 cm, Pieces 1A and B, 5, and 6: Limestone with glass clasts (1–3 cm in diameter). Limestone shows dark "dendritic" pattern (MnO or Mn[OH] n). Glass clasts are slightly altered to very pale brown (10YR 8/4) palagonite around the rims and within the cracks.

15–33 and 40–43 cm, Pieces 2, 3, 4, and 6): Black (10YR 2.5/1) glass, relatively fresh and uncracked; some fractures, however, are observed and subsequent palagonitization has occurred. Vesicles are found throughout (1–3 mm in diameter).

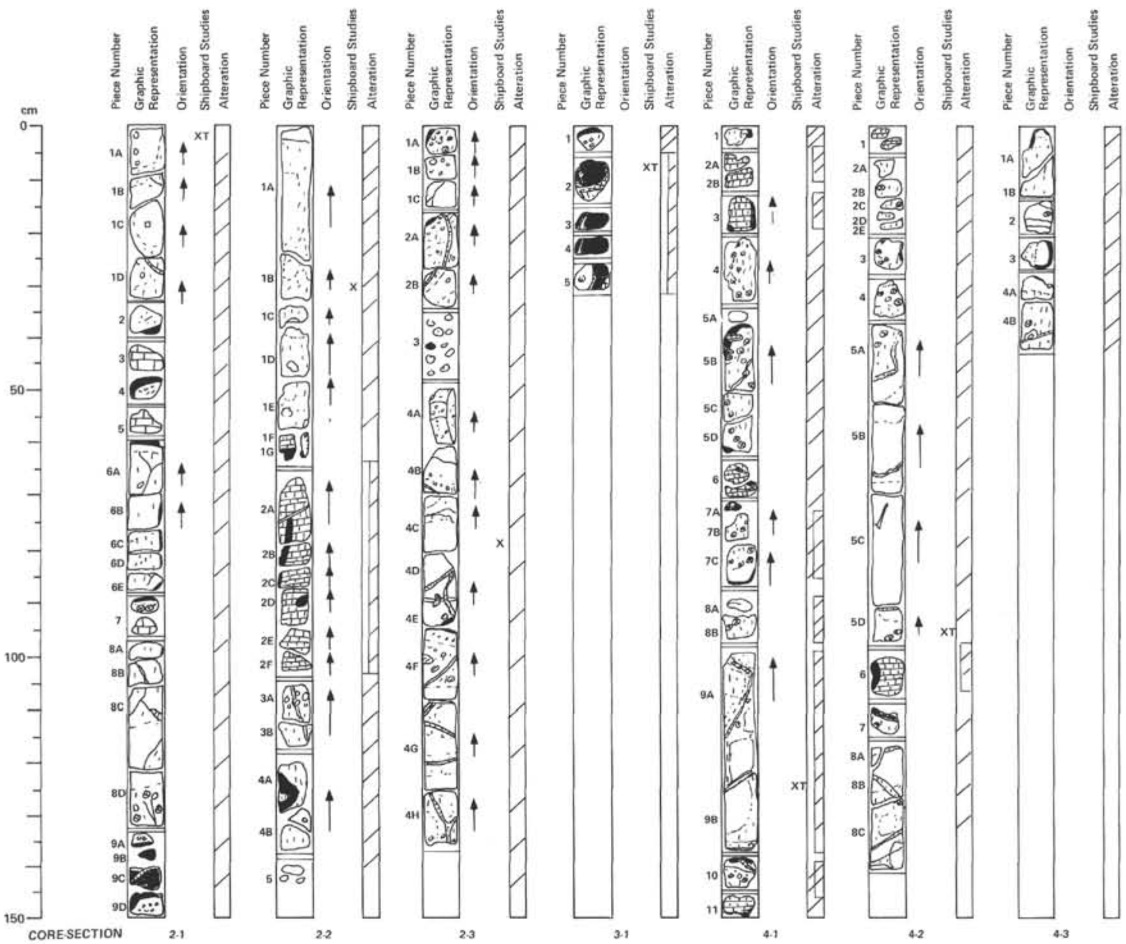

SITE 559, CORE 2 Depth 247.0–256.0 m

SECTION 1

APHYRIC PILLOW BASALT

0–147 cm: Dominantly aphyric dark gray (10YR 4/1) basalt. Fine grained. Grading through variolitic to black aphanitic basalt approaching glassy pillow margins. Largely altered dark grayish brown (10YR 4/2) to brown (10YR 5/3). Sparsely vesicular with small, round, unfilled vesicles (1–2%) concentrated (~5%) near pillow margins. *Scattered irregular larger vesicles (~5 mm) generally calcite filled.*

Limestone (46, 64–58, and 93–95 cm). Interpillow sediment: very pale brown (10YR 7/3) limestone generally with black MnO dendrites.

Basalt glass (135–145 cm). Thick rinds black, sparsely vesicular glass with black aphanitic basalt. Only weakly palagonitized.

SECTION 2

APHYRIC PILLOW BASALT AND LIMESTONE

0–64 and 104–140 cm: Aphyric pillow basalt, moderately/highly altered. Altered to brown (10YR 5/3) (highly altered) grading to dark grayish brown (10YR 4/2) (moderately altered). In 0–64 cm cores of less altered aphyric aphanitic basalt pillows; dark gray (7.5YR N4/0) to very dark gray (7.5YR N5/0). Vesicles throughout section, two generations possible: large, calcite filled (3–7 mm) and small, empty (<1–2 mm). Larger vesicles are concentrated in the highly altered upper sections of Pieces 1A and 3A, and a few in 4B; smaller vesicles are scattered.

60–102 cm: Limestone with glass clasts. 1–3 cm in length. Bioturbation is faint but present in majority of limestone pieces. Piece 1G is limestone with glass fragment 63.0–64.5 cm. Glass is black (10YR 2.5/1). Limestone grades from very pale brown (10YR 8/3) to light gray (10YR 7/2).

SECTION 3

APHYRIC PILLOW BASALTS

Aphyric, fine grained basalt as in Section 1. No interpillow limestone recovered. Calcite veining present as shown (diagonal hatched). Vesicle abundance increasing downhole. Small (< 2 mm) round, generally unfilled vesicles sparsely distributed throughout concentrated to 5–10% near upper pillow margins (shown by small dots and circles). Large, irregular, calcite filled vesicles (up to 5%), concentrated near upper pillow margins. Shown thus: or .

SITE 559, CORE 3 Depth 256.0–256.5 m

SECTION 1

BASALTIC PILLOW RIM PIECES

0–5 cm: Aphyric fine grained basalt altered grayish brown (10YR 6/2).

5–30 cm: Black basalt glass grading through black, aphanitic, sparsely vesicular basalt to grayish brown (10YR 6/2) variolitic basalt. Palagonite rims on exterior and fractured surfaces range from 1–4 mm thick.

Limestone (11–13 and 28–30 cm): brown (7.5YR 5/2) limestone filling interpillow voids.

SITE 559, CORE 4 Depth 256.5–265.0 m

SECTION 1

APHYRIC PILLOW BASALT, INTERPILLOW LIMESTONE

0–4, 24–62, and 70–144 cm: Aphyric pillow basalt sequence: black glass, rims (10YR 2.5/1) grading into black aphanitic, aphyric basalt (same color). Aphanitic basalt grades into variolitic basalt. Small, empty vesicles (<1 mm–1 mm in diameter) are present through this zone (aphanitic/variolitic), demarcating pillow interfaces. Variolitic to aphyric altered basalt ranges in color from yellowish brown (10YR 5/6) to grayish brown (10YR 5/8). Within this brown altered basalt are found larger vesicles (2–7 mm in length) filled with calcite; some cavities within calcite veins are lined with sparry calcite. In some pieces, unaltered dark gray (10YR 4/1) cores of unaltered aphanitic aphyric basalt are observed set within the brown altered basalt.

5–22, 64–69, and 146–150 cm: Limestone with glass clasts. Limestone ranges in color from brownish yellow (10YR 6/8) at 5–8 cm to very pale brown (10YR 8/4) at 8–12 cm to white (10YR 8/2) at 12–22 cm to very pale brown (10YR 8/3) at 64–69 cm to light gray (10YR 7/1) at 146–150 cm. Dendritic patterns (of Mn-Oxides or hydroxides?)
are present in all pieces. Glass is palagonitized along cracks and edges.

SECTION 2

APHYRIC PILLOW BASALT, INTERPILLOW LIMESTONE

0–5 and 99–106 cm: Limestone as in Section 1. Piece 6 contains a large glass fragment. Palagonitized along fracture joints and edges.

6–96 and 108–139 cm: Aphyric pillow basalt sequence as in Section 1. (Less total glass on aphyric basalt as compared to Section 1.) Vesicles pattern the same, all but fewer large vesicles about calcite veins. Gradation of brown altered basalt to cores of unaltered basalt is less clear than in Section 1; much more subtle and fuzzy.

SECTION 3

APHYRIC PILLOW BASALT

0–42 cm: Aphyric pillow basalt sequence as in Section 1. Aphanitic basalt borders are very clear as compared to Section 2.

SITE 559 HOLE CORE 2 CORED INTERVAL 247.0–256.0 m

TIME – ROCK UNIT	BIOSTRATIGRAPHIC ZONE	FOSSIL CHARACTER: FORAMINIFERS	NANNOFOSSILS	RADIOLARIANS	DIATOMS	SECTION	METERS	GRAPHIC LITHOLOGY	DRILLING DISTURBANCE	SEDIMENTARY STRUCTURES	SAMPLES	LITHOLOGIC DESCRIPTION
						1	0.5, 1.0	Basalt; Basalt				basalt 10YR 8/3 10YR 8/3
						2						10YR 7/3 10YR 7/3
						3		Basalt				
						4						10YR 6/3

INTRAPILLOW-BASALT (VOLCANICLASTIC) LIMESTONE

Very pale brown (10YR 8/3) to pale brown (10YR 6/3)

Volcaniclasts are rare

Manganese mineralization occurs throughout the limestone as micronodules and dendrites

Limestones are veined by sparry calcite.

Section 2, 60–102 cm: Moderately bioturbated limestone is in scoured contact (dip ~30°) lighter colored limestone

SITE 559 HOLE CORE 4 CORED INTERVAL 256.5–265.0 m

TIME – ROCK UNIT	BIOSTRATIGRAPHIC ZONE	FOSSIL CHARACTER: FORAMINIFERS	NANNOFOSSILS	RADIOLARIANS	DIATOMS	SECTION	METERS	GRAPHIC LITHOLOGY	DRILLING DISTURBANCE	SEDIMENTARY STRUCTURES	SAMPLES	LITHOLOGIC DESCRIPTION
						1	0.5, 1.0	Basalt				basalt 10YR 8/3–10YR 7/8 5YR 7/1
						2		Basalt; Basalt				5YR 7/1–5YR 8/2
						3						

INTRAPILLOW-BASALT (VOLCANICLASTIC) LIMESTONE

Colors vary from yellow (10YR 7/8), very pale brown (10YR 8/3) to light gray (5YR 7/1) and pinkish white (5YR 8/2)

Moderately bioturbated

Manganese mineralization occurs as dendrites and veins

Calcite veining common

Volcaniclasts are more common near pillow margins

SITE 559 HOLE CORE 5 CORED INTERVAL 265.0–274.0 m

TIME – ROCK UNIT	BIOSTRATIGRAPHIC ZONE	FOSSIL CHARACTER: FORAMINIFERS	NANNOFOSSILS	RADIOLARIANS	DIATOMS	SECTION	METERS	GRAPHIC LITHOLOGY	DRILLING DISTURBANCE	SEDIMENTARY STRUCTURES	SAMPLES	LITHOLOGIC DESCRIPTION
						1	0.5, 1.0	Basalt				Piece No. 4 5YR 8/2
						2		Basalt				
						3						

INTRAPILLOW-BASALT (VOLCANICLASTIC) LIMESTONE

Pinkish white (5YR 8/2) with manganese mineralization as black flecks possibly (doubtful) bioturbated.

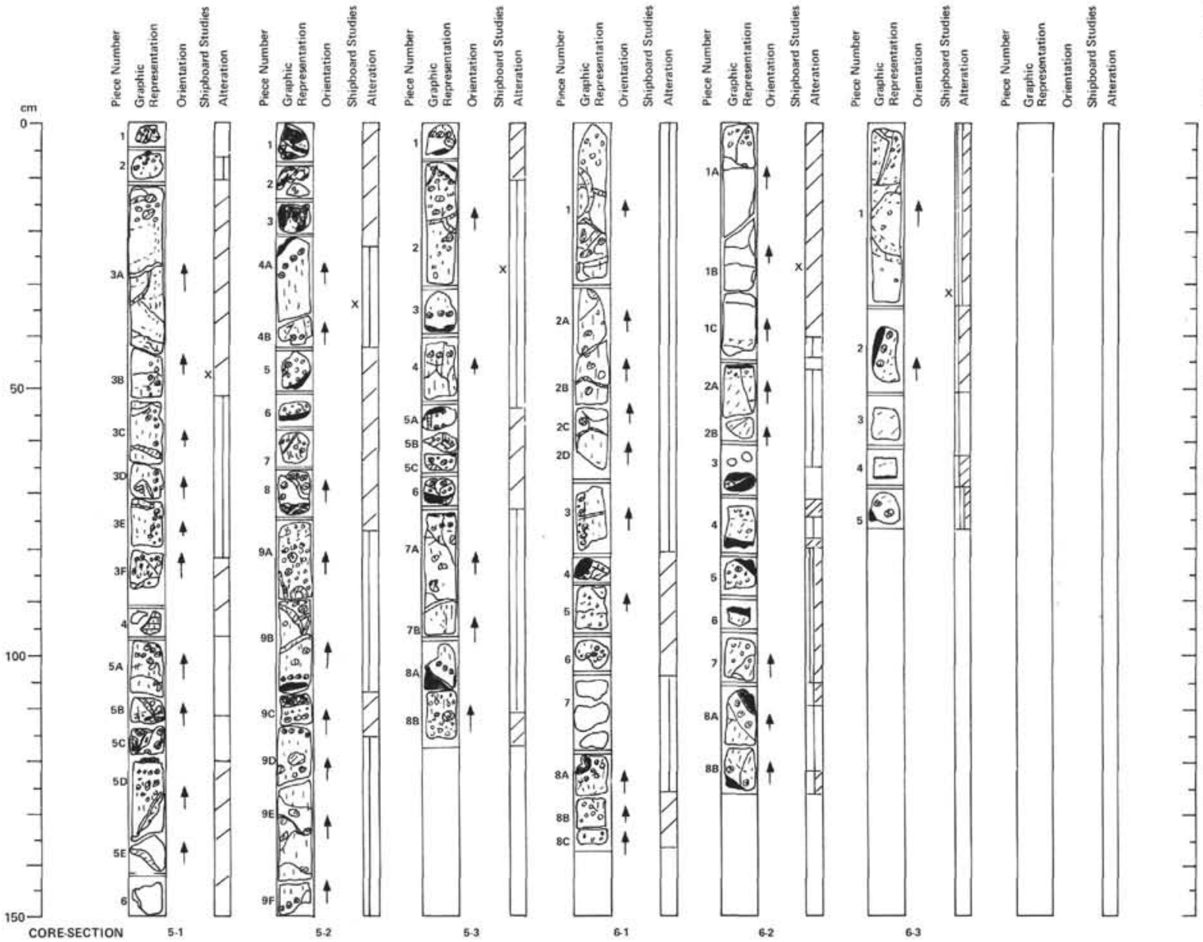

SITE 559, CORE 5 — Depth 265.0–274.0 m

SECTION 1

APHYRIC PILLOW BASALT

4–90, 98–112, and 118–145 cm: Aphyric basalt pillows ranging from moderately altered (gray – 10YR 5/1) to highly altered (pale brown – 10YR 6/3). Variolitic texture grading to black aphanitic basalt grading to glass rims in some cases (black on diagram). In aphanitic basalt: rounded empty vesicles (1–2 mm).

14–20 and 119–126 cm: Rounded and irregular calcite filled vesicles (1–2 mm, some up to 1 cm) in the variolitic part. Minor calcite veining throughout.

1–4 and 112–118 cm: Mostly fresh glass clasts (with palagonitized rims) in pinkish gray (7.5YR 6/2) limestone matrix.

90–98 cm: One piece of pinkish gray (7.5YR 7/2) limestone with fine dendritic black pattern (MnO?) and mostly altered glass clast.

SECTION 2

APHYRIC PILLOW BASALT

23–150 cm: Aphyric pillow basalts as in Section 1. Round, empty vesicles (1–2 mm) in black aphanitic basalt.

78–88 cm: Round and irregular vesicles (1–2 mm up to 1 cm).

113–124 cm: Filled with calcite in the more altered cores of the pillows and top variolitic edges.

56–58, 71–72, 76–78, and 104–110 cm: Mostly fresh black glass rims with calcite veining and some alteration to clays grading into black aphanitic basalts (filled with rounded empty vesicles).

0–20 cm: Fresh and moderately altered glass in minor limestone matrix with minor calcite veining.

SECTION 3

APHYRIC PILLOW BASALT

As in Sections 1 and 2.

5–12 cm, 39–40, 70–77, and 101–104 cm: Glass rims grading to black aphanitic basalt (some with rounded, *empty (1–3 mm) vesicles as in Sections 1 and 2) and variolites.*

111–119, 46–47, 80–89, and 106–115 cm: Rounded to irregular calcite vesicles (1–2 mm up to 1.2 cm) in more altered upper variolitic edges of pillows.

SITE 559, CORE 6 — Depth 274.0–283.0 m

APHYRIC PILLOW BASALT

Similar to Core 5. Moderately–heavily altered aphyric basalt ranging from dark gray (10YR 4/1) through grayish brown (10YR 5/2) to brown (10YR 5/3). Several areas grading from altered core through variolitic texture through black aphanitic basalt and some glass rims rounded to irregular calcite-filled (1–2 mm up to 1 cm) vesicles in altered parts. Rounded empty (1–3 mm) vesicles in black aphanitic basalt. Minor calcite veining in fractures throughout section.

SECTION 2

APHYRIC PILLOW BASALT

Moderately to badly altered, fine grained aphyric basalt; color dark gray (10YR 4/1) to brown (10YR 5/3). Vitric cooling margins occur at 46–47, 65–70, 78–84, 90–92, 105–110, and 122–124 cm. Some pieces show variolitic transition to interior of pillows. Two kinds of vesicles are occurring: a) round shaped (size <2 mm); and b) irregular shaped (size <10 mm); if vesicles are located in fresher parts of the basalt, they are mostly empty, otherwise filled with calcite. Fractures and veinlets are usually filled with calcite, too.

SECTION 3

APHYRIC PILLOW BASALT

Same description as Section 2.

Moderately to badly altered aphyric, fine grained basalt with some glass margins (Pieces 2, 4, and 5). Variolites in Pieces 2 and 5.

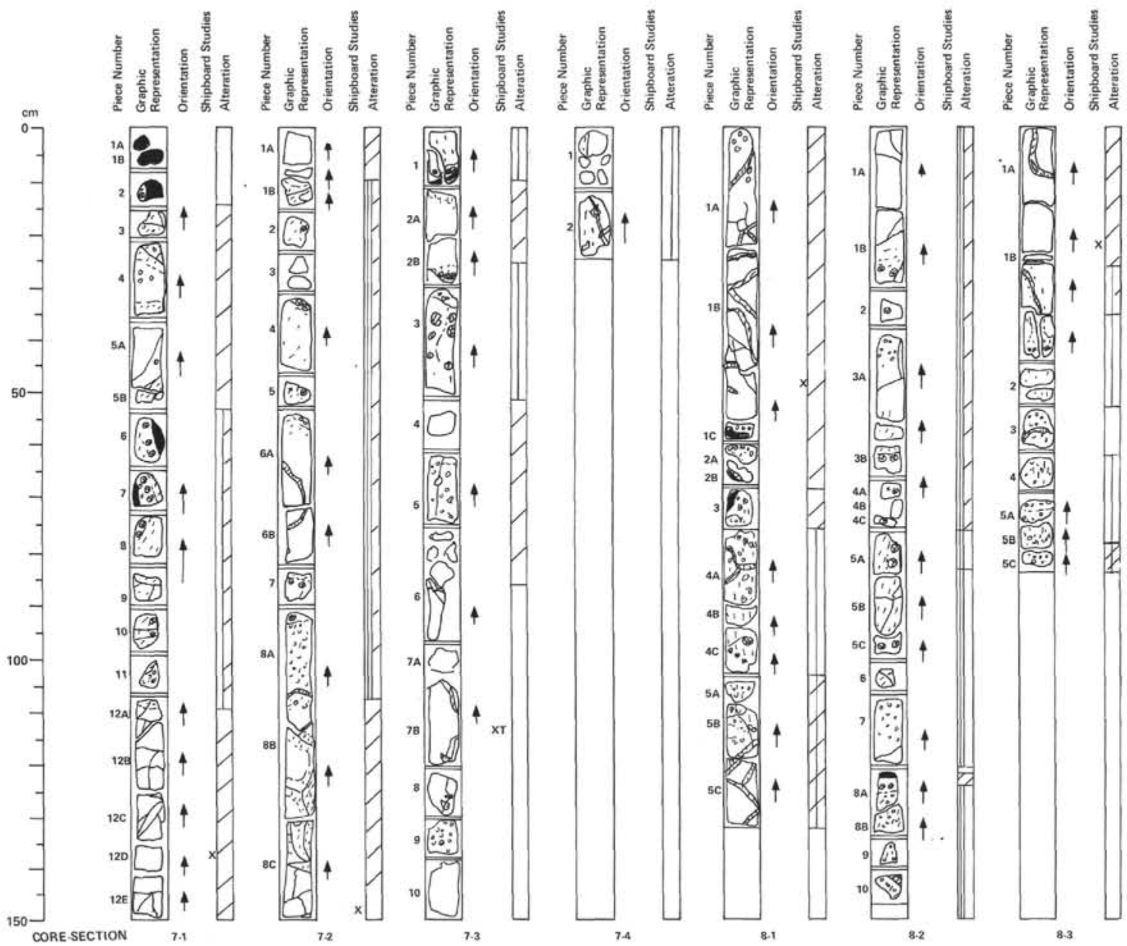

SITE 559, CORE 7 Depth 283.0–292.0 m

SECTION 1

APHYRIC PILLOW BASALT

0–14 cm: Black glass and aphanitic basalt. Vesicles are common and mostly empty. Veinlets are filled with calcite. Piece 2 shows some varioles. (Size of vesicles < 1.5 mm, size of varioles <2 mm).

16–150 cm: Fine grained, aphyric basalt; color dark gray (2.5Y N4/0) to dark grayish brown (2.5Y 4/2) in altered regions close to fractures and (calcite filled) veinlets. Two different kinds of vesicles occur: a) round, <1.5 mm and b) irregular, <1.2 cm. They are mostly filled with calcite.

54–80 cm: Pieces show variolitic transition from fine grained to aphanitic basalt.

SECTION 2

1–150 cm: Aphyric pillow basalt. Fine grained, moderately to badly altered. Color dark gray (2.5Y N4/0) to dark grayish brown (2.5Y 4/2). Variolitic texture in Pieces 2, 4, 5, 6, 7, and 8.

91–105 cm: Basalt is highly vesicular: a) round vesicles < 2 mm are filled with calcite in altered part of rock, in aphanitic part empty; and b) irregular vesicles <8 mm are filled with calcite.

SECTION 3

APHYRIC PILLOW BASALT

0–12 cm: Moderately altered, gray (2.5Y N5) aphyric fine grained basalt with glass chill margin of 10 cm (as in Sections 1 and 2).

New Unit:

120–150 cm: Coarser grained (but still fine) yellowish gray (5Y 5/1), aphyric basalt with very fine (≤3 mm) visible plagioclase needles and very small (< 0.5 mm) equant grains that are olive brown to reddish brown = olivine(?). Upper part (10–85 cm) is moderately altered, lower part (85–150 cm) is fresher.

33–42 and 63–74 cm: 5% round and irregular calcite filled vesicles (≤3 mm) in altered part; and 2% round empty vesicles in aphanitic basalt margin and also in altered part near margin.

131–136 cm: 5% round (≤2 mm) calcite filled vesicles and <1% round (≤2 mm) empty vesicles on edge of rock.

SECTION 4

APHYRIC PILLOW BASALT

Highly altered continuation of fine grained, aphyric basalt starting at Section 3, 12 cm.

SITE 559, CORE 8 Depth 292.0–301.0 m

SECTION 1

APHYRIC PILLOW BASALT

0–54 and 69–132 cm: Fine grained (coarser grained than previous unit), slightly to moderately to heavily (79–103 cm) altered, aphyric basalt as in Section 3, 12 cm and Section 4.

54–79 cm: Black aphanitic basalt with glass chill margins and 2% round, empty (<2 mm) vesicles. There is more fracturing (calcite filled) in Core 8, Section 1 than Core 7, Sections 3 and 4.

79–86 and 105–113 cm: 5% round and irregular (≤3 mm) calcite filled vesicles in altered parts of pillows.

SECTION 2

0–145 cm: Aphyric pillow basalt. Moderately to badly altered, fine grained. Partly variolitic transition from altered inner part to fresher aphanitic part (rim) of pillow. Glass occurs at 77–83 and 121–123 cm. Round vesicles (filled with calcite in altered regions of rock) are common at 39–~45 and 107–145 cm (size < 3.5 mm). Color of basalt dark gray to dark grayish brown (2.5Y N4/0 to 2.5Y 4/2).

SECTION 3

APHYRIC PILLOW BASALT

Same unit and characteristics as in Sections 1 and 2 with usual calcite-filled vesicles in altered part of rock (63–67 and 75–82 cm).

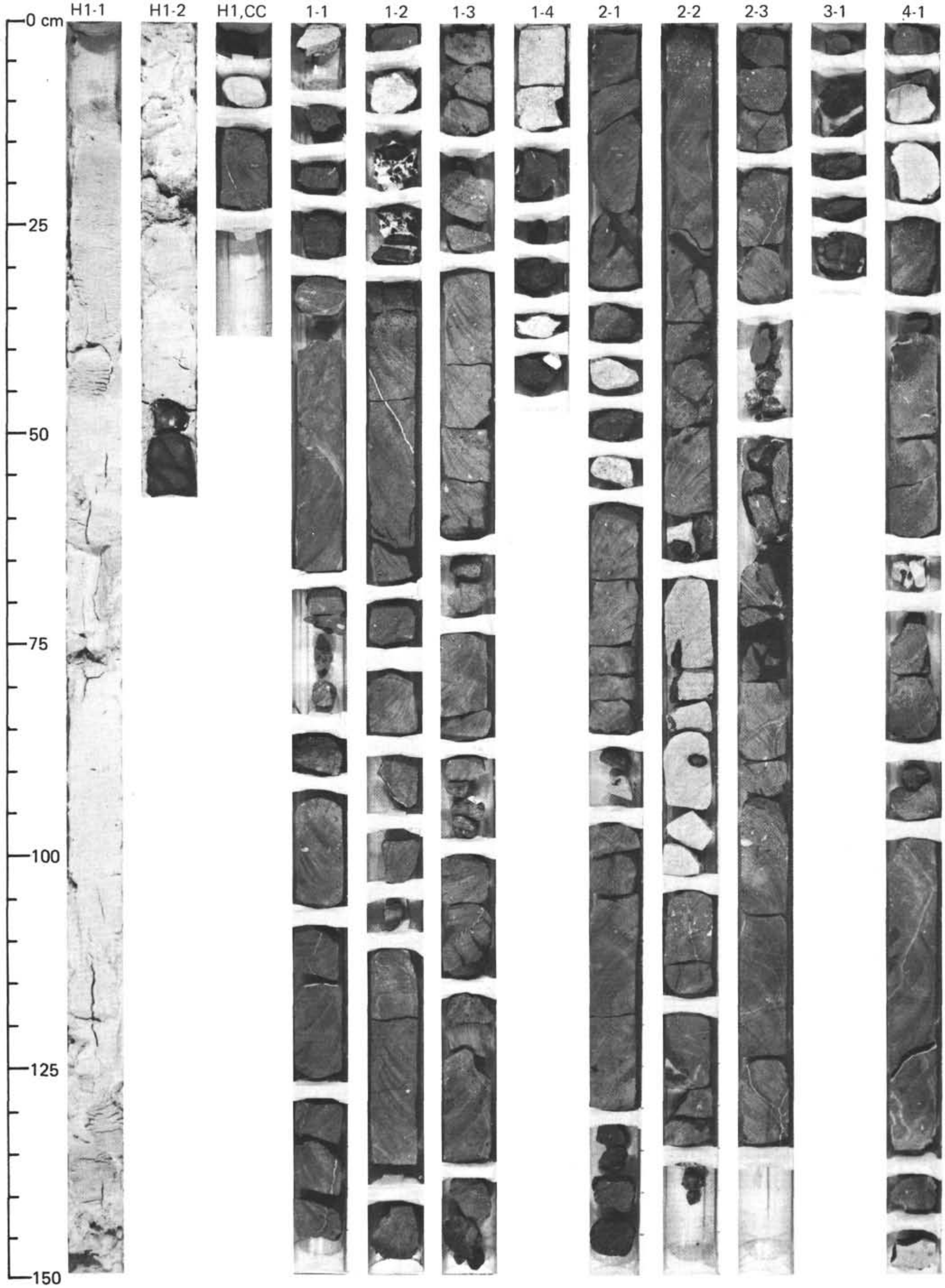
H1-1
H1-2
H1,CC
1-1
1-2
1-3
1-4
2-1
2-2
2-3
3-1
4-1
0 cm
25
50
75
100
125
150

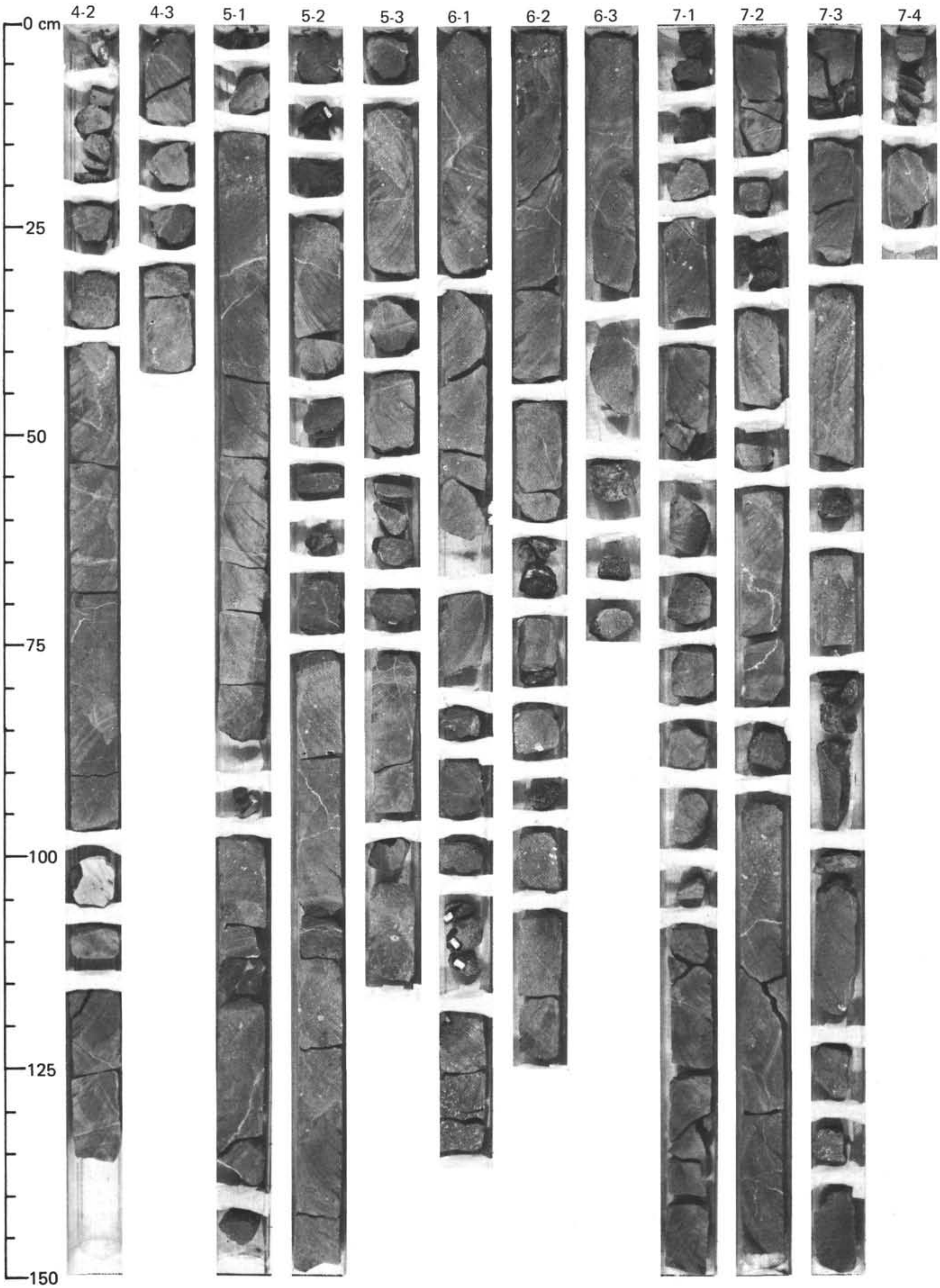
0 cm
25
50
75
100
125
150
4-2
4-3
5-1
5-2
5-3
6-1
6-2
6-3
7-1
7-2
7-3
7-4

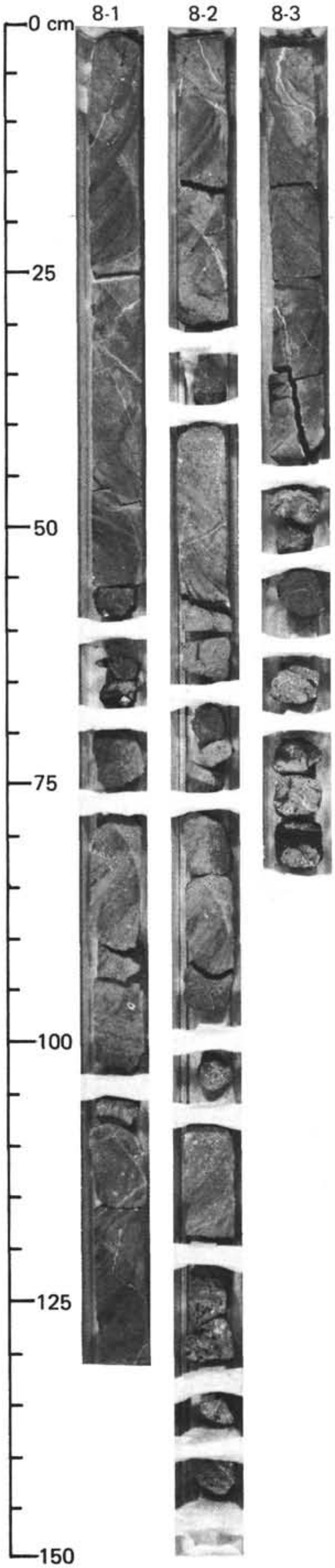
8-1
8-2
8-3
0 cm
25
50
75
100
125
150